Chemical Science

EDGE ARTICLE

View Article Online
View Journal | View Issue

Cite this: *Chem. Sci.*, 2019, **10**, 2186

All publication charges for this article have been paid for by the Royal Society of Chemistry

Efficient solar cells sensitized by a promising new type of porphyrin: dye-aggregation suppressed by double strapping†

Kaiwen Zeng,[a] Yunyue Lu,[a] Weiqiang Tang,[b] Shuangliang Zhao,[b] Qingyun Liu,[c] Weihong Zhu,[a] He Tian[a] and Yongshu Xie *[a]

Received 7th November 2018
Accepted 13th December 2018

DOI: 10.1039/c8sc04969f

rsc.li/chemical-science

Porphyrin sensitizers play essential roles in the development of efficient dye-sensitized solar cells (DSSCs). To further improve power conversion efficiency (PCE), it is vital to reduce undesirable dye aggregation that causes serious charge recombination and lowered open-circuit voltages (V_{oc}). To this end, we herein report a new class of porphyrin-based dyes **XW40** and **XW41**, with the porphyrin cores strapped with two circle chains. Compared with the reference sensitizer **XW10** which contains a porphyrin core wrapped in four dodecoxyl chains, the double strapping in **XW40** not only effectively suppresses the dye aggregation but also improves the dye loading amount. As a result, the V_{oc} and photocurrent (J_{sc}) were improved by 19 mV and 0.8 mA cm^{-2}, respectively, compared with the corresponding values of **XW10**, and the efficiency was improved from 8.6% obtained for **XW10** to 9.3% for **XW40**. To further extend the spectral response, an electron-withdrawing benzothiadiazole (BTD) unit was introduced as an auxiliary acceptor in **XW41**. Impressively, the onset wavelength of its IPCE spectrum was dramatically red-shifted to 830 nm. However, the extended π-conjugation framework results in aggravated dye aggregation, and thus a lowered efficiency of 8.2% was obtained for **XW41**. Through a combined approach of coadsorption and cosensitization, the efficiencies were dramatically enhanced to 10.6% and 10.2% for **XW40** and **XW41**, respectively, as a result of simultaneously enhanced V_{oc} and J_{sc}. The results of this work provide a novel strategy for developing efficient DSSCs by employing strapped porphyrin dyes.

Introduction

Because of the increasingly serious energy shortage problems associated with the exhaustion of fuel energy resources, inexhaustible clean energy sources are highly desired. In this respect, solar energy has been considered as the most viable option for sustainable development of human society. Among the photovoltaic devices, dye-sensitized solar cells have drawn considerable attention over the past two decades, showing advantages of relatively low-cost, eco-friendliness, and relatively high PCE.[1] Since Grätzel and coworkers first reported a ruthenium dye based DSSC with a PCE of 7.1% in 1991,[2] numerous efforts have been devoted to improve cell efficiency. For this purpose, porphyrin and their derivatives have been developed as promising sensitizers because of their facile structural modification and intrinsic strong absorption capability, showing an intense Soret band and moderate Q bands in the ranges of 400–450 nm and 550–650 nm, respectively.[3–5]

Highly efficient porphyrin sensitizers usually feature a donor–π–acceptor (D–π–A) configuration.[6] Such structures exhibit excellent intramolecular charge transfer (ICT) properties, and tunable optical, physical and electrochemical properties.[7] However, simple porphyrin dyes usually exhibit poor absorption in the near infrared (NIR) region. To enhance light-harvesting ability in the NIR region, porphyrin sensitizers with extended conjugation frameworks have been developed.[8–10] However, this approach usually aggravates the undesired dye aggregation, which may result in serious charge recombination, low electron-injection efficiency, and poor cell performance.[11–15] To overcome such a problem, efficient porphyrin dyes have been developed by wrapping the porphyrin macrocycle with four *o*-alkoxyl moieties on the *meso*-phenyl substituents.[16–20] In this respect, we have designed **XW10** using a phenothiazine-based donor, and an efficiency of 8.6% was achieved for the individual dye.[33]

On the basis of **XW10**, with the purpose of further suppressing the dye aggregation effect, we herein report a new class of porphyrin sensitizers **XW40** and **XW41** (Fig. 1) with double

[a]*Key Laboratory for Advanced Materials and Feringa Nobel Prize Scientist Joint Research Center, School of Chemistry and Molecular Engineering, East China University of Science &Technology, 130 Meilong, Shanghai 200237, China. E-mail: yshxie@ecust.edu.cn*

[b]*School of Chemical Engineering and State Key Laboratory of Chemical Engineering, East China University of Science and Technology, Shanghai, 200237, China*

[c]*College of Chemical and Environmental Engineering, Shandong University of Science and Technology, Qingdao, P. R. China*

† Electronic supplementary information (ESI) available. See DOI: 10.1039/c8sc04969f

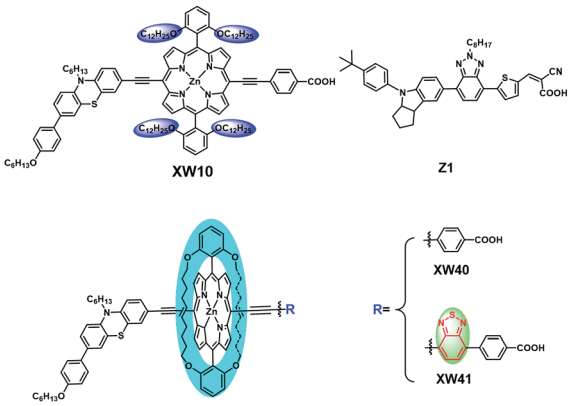

Fig. 1 Molecular structures of the porphyrin dyes and the cosensitizer **Z1**.

straps. Compared with **XW10**, the straps in **XW40** are favourable for suppressing dye aggregation, resulting in simultaneously improved V_{oc} and J_{sc} and an efficiency of 9.3%, obviously higher than the 8.6% obtained for **XW10**. On this basis, **XW41** was synthesized by introducing an auxiliary benzothiadiazole (BTD) moiety with the purpose of further extending the absorption spectrum.[9,21–24] As a result, the onset wavelength of photocurrent response was red-shifted to 830 nm. Upon cosensitization with an organic dye, **Z1**, high efficiencies of 10.6% and 10.2% were achieved for **XW40** and **XW41**, respectively, based on the traditional iodine electrolyte. Although circle chain strapping has been demonstrated to be effective in developing organic dyes,[25,26] and strapped porphyrins have been reported for fabrication of OLEDs, and to achieve charge transfer and sensitization behavior on semiconductor films,[27–29] this approach has not yet been employed in designing efficient porphyrin dyes. The results of this work provide an effective novel strategy for designing efficient porphyrin dyes by introducing double straps.

Results and discussion

Synthesis of dyes

The synthesis routes are depicted in Scheme 1 and Scheme S1.† 2,6-bis(Hex-5-en-1-yloxy)benzaldehyde **1** was prepared from commercially available 2,6-dihydroxybenzaldehyde in 92% yield. Acid-catalysed condensation of **1** with dipyrromethane followed by DDQ oxidation provided 5,15-bis(2,6-bis(hex-5-en-1-yloxy)phenyl)porphyrin **2**. Bromination of **2** with NBS followed by Zn^{II}-ion insertion gave porphyrin **4**, which was subjected to ring-closing metathesis (RCM) using the second-generation Grubbs catalyst, affording the key intermediate doubly strapped porphyrin **5**. Then, it was successively reacted with the ethynyl derivatives of phenothiazine, and the acid ester of the acceptor through Sonogashira reactions to introduce the donor and the acid ester of the acceptor, respectively, in the *meso*-positions of the strapped porphyrin framework. Finally, the target dyes were obtained through hydrolysis of the corresponding esters. All the compounds were systematically characterized by ^{1}H NMR, ^{13}C NMR, and mass spectrometry (HRMS; ESI†). In addition, the key

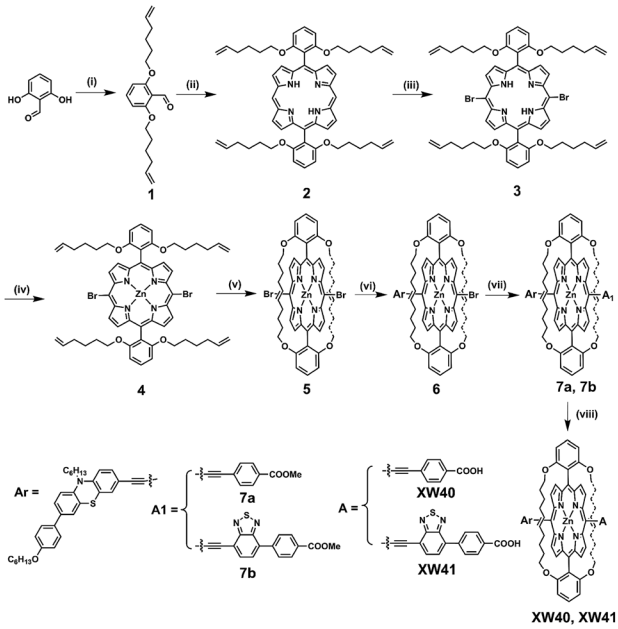

Scheme 1 Synthetic routes to sensitizers **XW40** and **XW41**. Reaction conditions: (i) 6-bromo-1-hexene, K_2CO_3, DMF; (ii) TFA, DDQ, Et_3N, CH_2Cl_2; (iii) NBS, CH_2Cl_2; (iv) $Zn(OAc)_2\cdot 2H_2O$, CH_2Cl_2, CH_3OH; (v) 2nd generation Grubbs catalyst, CH_2Cl_2; (vi) 3-ethynyl-10-hexyl-7-(4-(hexyloxy)phenyl)-10*H*-phenothiazine, $AsPh_3$, $Pd_2(dba)_3$, THF, Et_3N; (vii) for **7a**: methyl-4-ethynylbenzoate, $Pd_2(dba)_3$, $AsPh_3$, Et_3N, THF; for **7b**: methyl 4-(7-ethynylbenzo[*c*][1,2,5]thiadiazol-4-yl)benzoate, $Pd_2(dba)_3$, $AsPh_3$, Et_3N, THF; and (viii) $LiOH\cdot H_2O$, THF, H_2O.

intermediate **5** was further characterized with single crystal X-ray diffraction analyses (Fig. S4†).

Spectral properties

The electronic absorption spectra of the dyes in THF are shown in Fig. 2, and the corresponding absorption together with emission data are listed in Table 1.

As expected, all the porphyrin dyes exhibit a typical intense Soret band around 460 nm and less intense Q bands in the wavelength range of 600–750 nm. Compared with **XW10**, doubly

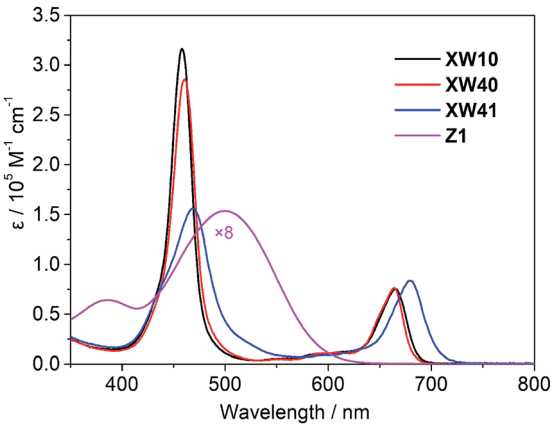

Fig. 2 Absorption spectra of the porphyrin dyes and the cosensitizer **Z1** in THF.

Table 1 Absorption spectral and electrochemical data for XW40, XW41 and Z1

Dye	λ_{max}/nm ($\varepsilon/10^5$ M^{-1} cm^{-1})[a]	λ_{max}/nm[b]
XW10[33]	459 (316), 591 (10.4), 666 (75.2)	676
XW40	461 (286), 594 (10.9), 664 (76.6)	672
XW41	468 (156), 627 (14.3), 680 (83.7)	700
Z1	386 (8.03), 501 (19.2)	672

[a] Absorption peaks in THF (4×10^{-6} M). [b] Emission peaks in THF (4×10^{-6} M).

strapped porphyrin dye **XW40** exhibits slightly red-shifted Soret band, and its Q bands are almost identical to those of **XW10**. As expected, the introduction of an auxiliary benzothiadiazole (BTD) group in **XW41** dramatically improves the light-harvesting ability up to 730 nm.

The absorption spectra of **XW40** and **XW41** on 3 μm thick TiO_2 films are shown in Fig. S1.† Compared with the corresponding absorption spectra in THF, all the spectra acquired on the films show broadened absorption, beneficial for enhancing the light-harvesting ability, and the Q peaks are hypsochromically shifted, which can be ascribed to the deprotonation of the carboxylic acid moiety.[30–32] Notably, the weak blue shoulder of the Soret band observed for **XW10** was not discernible in **XW40**, indicating that the H-type aggregation of porphyrins on TiO_2 might be insignificant. However, the re-appearance of the obvious blue-shoulder of the Soret band in the **XW41**/TiO_2 spectrum indicates severe aggregation due to the introduction of the BTD group,[16,30] which is detrimental to DSSC photovoltaic performance.

Electrochemical studies

Cyclic voltammetry (Fig. S3†) was carried out to investigate the thermodynamic driving force of electron injection from the photoexcited dyes to the conduction band of TiO_2, and dye regeneration by the redox electrolyte. The obtained HOMO levels corresponding to the ground state oxidation potentials of the two dyes are 0.71 and 0.72 V (*vs.* NHE), respectively (Table 2). Their HOMO levels are well below the redox potential of the iodide/triiodide couple (~0.4 V *vs.* NHE), indicating thermodynamically feasible regeneration processes for the sensitizers, and the respective LUMO levels of −1.15 and −1.08 V for **XW40** and **XW41** lie well above the conduction band edge of TiO_2 (−0.5 V *vs.* NHE), indicating sufficient driving forces for the electron injection processes (Fig. 3).

Table 2 Electrochemical data and the energy levels of the molecular orbitals for the dyes adsorbed on TiO_2 films

Dyes	HOMO[a]/V (NHE)	E_{0-0}[b]/V	LUMO[c]/V (NHE)
XW40	0.71	1.86	−1.15
XW41	0.72	1.80	−1.08

[a] HOMO levels were obtained from the first oxidation potential measured in acetonitrile using 0.1 M tetrabutylammonium hexafluorophosphate ($TBAPF_6$) as the electrolyte (working electrode: FTO/TiO_2/dye; reference electrode: SCE; calibrated with ferrocene/ferrocenium (Fc/Fc$^+$) as an external reference. Counter electrode: Pt). [b] Estimated from the wavelength at the intersection (λ_{inter}) of normalized and emission spectra with the equation $E_{0-0} = 1240/\lambda_{inter}$. [c] The LUMO was calculated from the equation LUMO = HOMO − E_{0-0}.

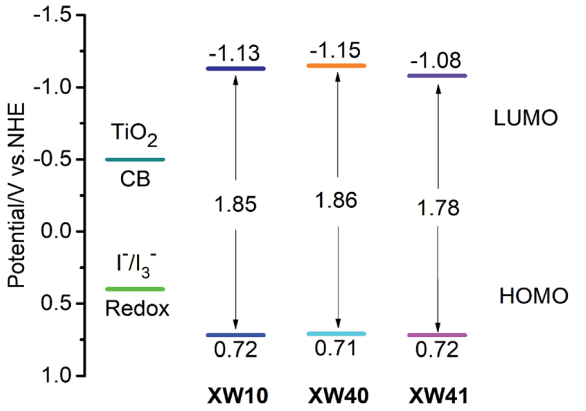

Fig. 3 Schematic energy-level diagram of XW10,[33] XW40 and XW41.

Theoretical calculations

To gain insight into the electron distribution of distinct porphyrin dyes, density functional theory (DFT) calculations were performed using the Gaussian 09 program package. As presented in Fig. 4, the HOMO orbitals of porphyrin dyes **XW40** and **XW41** are distributed over the phenothiazine donors and the porphyrin frameworks. The LUMO orbitals of **XW40** are predominantly delocalized over the acceptor and porphyrin moiety, while the LUMO orbitals of **XW41** are mainly delocalized over the porphyrin framework, the BTD unit and the carboxyphenyl acceptor. The obvious overlap between the HOMO and LUMO orbitals facilitates the efficient intramolecular charge-transfer from the donor to the acceptor and subsequent electron-injection from the excited dyes to the TiO_2 film.[34–36]

Photovoltaic performance

The porphyrin dyes were evaluated as the sensitizers for fabricating DSSCs based on the traditional I^-/I_3^- electrolyte. Fig. 5 shows the photocurrent–voltage (*J*–*V*) curves of the DSSCs, and the photovoltaic parameters are listed in Tables 3 and S1.†

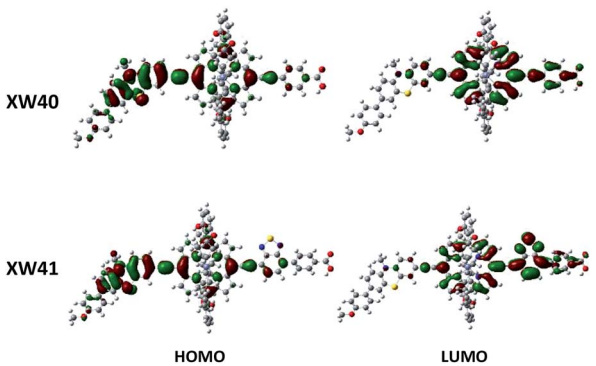

Fig. 4 Frontier molecular orbital profiles of XW40 and XW41.

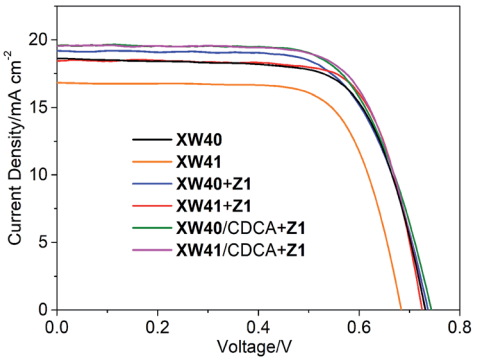

Fig. 5 J–V characteristics of the DSSCs based on **Z1**, **XW40** and **XW41**.

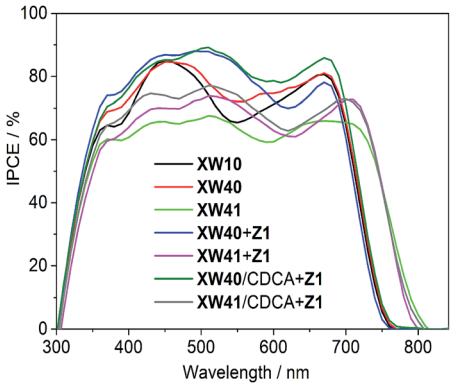

Fig. 6 IPCE action spectra for the DSSCs based on **XW10**,[33] **Z1**, **XW40** and **XW41**.

The DSSCs based on **XW40** exhibit a PCE of 9.3%, higher than the 8.6% obtained for **XW10**, with V_{oc} and J_{sc} improved to 730 mV and 18.90 mA cm^{-2}, respectively, compared to the respective values of 711 mV and 17.90 mA cm^{-2} obtained for **XW10**.[33] These observations indicate that the porphyrin core strapping is favorable for suppressing the aggregation effect and reducing the charge recombination, and thus the V_{oc} of **XW40** was significantly enhanced by 19 mV, compared to that of **XW10**. On the other hand, the J_{sc} of **XW40** was also improved despite the fact that **XW40** and **XW10** possess identical π-conjugation backbones and very similar absorption spectra. To further understand the enhancement of J_{sc}, we measured the adsorption amounts of the dyes (Table 3). The loading amount of **XW40** was found to be 1.99 × 10^{-7} mol cm^{-2}, 23% higher than the 1.62 × 10^{-7} mol cm^{-2} measured for **XW10**. Hence, the higher J_{sc} obtained for **XW40** can be rationalized by its larger dye adsorption amount, which may be ascribed to the fact that the doubly strapped porphyrin molecule may occupy a smaller area, because the doubly strapped structure is more compact than the quadruply wrapped structure. Compared to **XW40**, although **XW41** absorbs light over a broader range due to the presence of an extra BTD unit, it exhibits a lower PCE of 8.2%, which may be ascribed to the lower V_{oc} of 695 mV associated with the aggravated dye aggregation effect induced by the extended conjugation framework. However, the efficiency of **XW41** is still higher than the 7.8% obtained for **XW11**,[33] in agreement with the superior anti-aggregation abilities of the doubly strapped porphyrins relative to the quadruply wrapped porphyrins.

The incident photon-to-current conversion efficiency (IPCE) spectra for the dyes were also measured to probe the efficiencies for the conversion of the absorbed sunlight to electrical current at various wavelengths. As shown in Fig. 6, the bandwidths of IPCE spectra for **XW40** are almost the same as those of **XW10**,[33] but the plateau is slightly higher than that of **XW10**, which is consistent with the improved J_{sc}. Impressively, the introduction of the auxiliary BTD acceptor unit in **XW41** successfully expanded the light responsive wavelengths into the NIR region with a striking onset wavelength of 830 nm, but the plateau is obviously lowered, leading to a lowered J_{sc} of 16.77 mA cm^{-2}.

It is obvious that both **XW40** and **XW41** exhibit obvious valleys within 500–600 nm in the IPCE spectra. To fill up the valleys, an organic dye, **Z1** (Fig. 1, Table S2†), was thus synthesized and employed for co-sensitization with **XW40** and **XW41**.

Table 3 Photovoltaic parameters of the porphyrin DSSCs under AM1.5 illumination (power, 100 mW cm^{-2}). The active area is 0.12 cm^2

					Dye loading amount (× 10^{-7} mol cm^{-2})	
Dye	V_{oc}/mV	J_{sc}/mA cm^{-2}	FF	PCE (%)	Porphyrin	**Z1**
XW10[a]	711 ± 5	17.90 ± 0.04	0.684 ± 0.005	8.60 ± 0.10	1.62	\
XW40	730 ± 3	18.67 ± 0.75	0.683 ± 0.021	9.31 ± 0.12	1.99	\
XW41	695 ± 2	16.77 ± 0.31	0.701 ± 0.006	8.16 ± 0.10	2.78	\
Z1[b]	788 ± 3	13.30 ± 0.15	0.781 ± 0.004	8.23 ± 0.03	\	6.47
XW40 + **Z1**[c]	742 ± 1	19.36 ± 0.49	0.694 ± 0.013	9.97 ± 0.06	1.62	3.67
XW41 + **Z1**[c]	728 ± 3	18.32 ± 0.13	0.728 ± 0.003	9.71 ± 0.01	2.65	1.96
XW40/CDCA + **Z1**[d]	748 ± 2	19.59 ± 0.21	0.719 ± 0.004	10.55 ± 0.11	1.64	2.73
XW41/CDCA + **Z1**[d]	726 ± 2	19.63 ± 0.31	0.715 ± 0.003	10.19 ± 0.21	2.39	3.06

[a] The data were reported in our previous work.[33] [b] The measurement procedure was adapted from the reported work.[37] [c] The cosensitization was performed through an optimized stepwise approach: the TiO_2 electrode was first dipped in 0.2 mM porphyrin dye in chloroform/ethanol (v/v, 3/2) for 12 h, rinsed with ethanol, and then immersed in a 0.3 mM solution of **Z1** in chloroform/ethanol (v/v, 1/1) for 1.5 h (**XW40** + **Z1**) or 0.75 h (**XW41** + **Z1**). [d] The approach is similar to the simple cosensitization approach, except that the TiO_2 electrode was first dipped in a cocktail solution of porphyrin (0.2 mM) and CDCA (1.0 mM), then in **Z1** (0.3 mM) for 1.5 h for the optimized conditions.

Upon co-sensitization, the valleys in the IPCE spectra were filled up by the contribution from the absorption of **Z1**, and thus better photovoltaic performance was achieved for both **XW40** and **XW41**, with higher efficiencies of 10.0% and 9.7%, respectively, as a result of simultaneously improved J_{sc} and V_{oc}. The enhancement of J_{sc} can be readily rationalized by the fact that the IPCE spectra are obviously improved upon cosensitization. On the other hand, the improved V_{oc} values achieved for the cosensitization systems lie between the corresponding values obtained for the individual porphyrin dyes and the cosensitizer. These observations agree well with previous results of cosensitization systems.[33,38–40]

Generally, the utilization of CDCA as a coadsorbent is effective for suppressing dye aggregation and enhancing the photovoltaic performance. Hence, a combined strategy of coadsorption and cosensitization was employed with the purpose of further enhancing the photovoltaic performance of DSSCs. Thus, the DSSCs were fabricated by immersing TiO_2 films in a cocktail solution containing the individual porphyrin dye and CDCA for 12 h, followed by dipping in a solution containing **Z1**. Compared with **XW40** + **Z1** and **XW41** + **Z1**, the J_{sc} values obtained for **XW40**/CDCA + **Z1** and **XW41**/CDCA + **Z1** were improved to 19.59 and 19.63 $mAcm^{-2}$, respectively, with the efficiencies enhanced to 10.6% and 10.2%, respectively. The improved J_{sc} values are consistent with the improved IPCE responses (Fig. 6). As we know, the presence of CDCA can suppress dye aggregation, decrease the rate of aggregation-induced non-radiative energy transfer, enhance electron injection yield, and thus improve the IPCE response.[7] For **XW40**/CDCA + **Z1**, the improved IPCE response around 500 nm was offset by the decreased loading amount of **Z1** which features a broad absorption around 500 nm (Fig. S5†). Meanwhile, the loading amount of **XW40** remains almost unchanged. As a result, the IPCE response was improved mainly in the Q band region. For **XW41**/CDCA + **Z1**, the loading amounts of **XW41** and **Z1** were decreased and increased, respectively, compared with the corresponding values for the cells based on **XW41** + Z1. Consistently, the IPCE response was improved mainly within the wavelength range of 400–600 nm.

Electrochemical impedance spectroscopy analysis

The V_{oc} for a DSSC is dependent on the TiO_2 conduction band edge (E_{CB}) and the charge recombination process, which can be inferred from the chemical capacitance (C_μ) and electron lifetime (τ), respectively. To provide further insight into the improved photovoltaic behavior of the doubly strapped porphyrin dyes, electrochemical impedance spectroscopy (EIS) was conducted under dark conditions. Thereby, the C_μ and τ values were obtained through fitting the EIS spectra.

As shown in Fig. 7a, the devices based on **XW40** showed similar C_μ values with those of **XW10** at a given V_{oc}. However, the electron lifetimes of **XW40** were found to be obviously longer than those of **XW10** (Fig. 7b), indicating a slower interfacial charge recombination process, which is consistent with the significantly enhanced V_{oc} for the doubly strapped

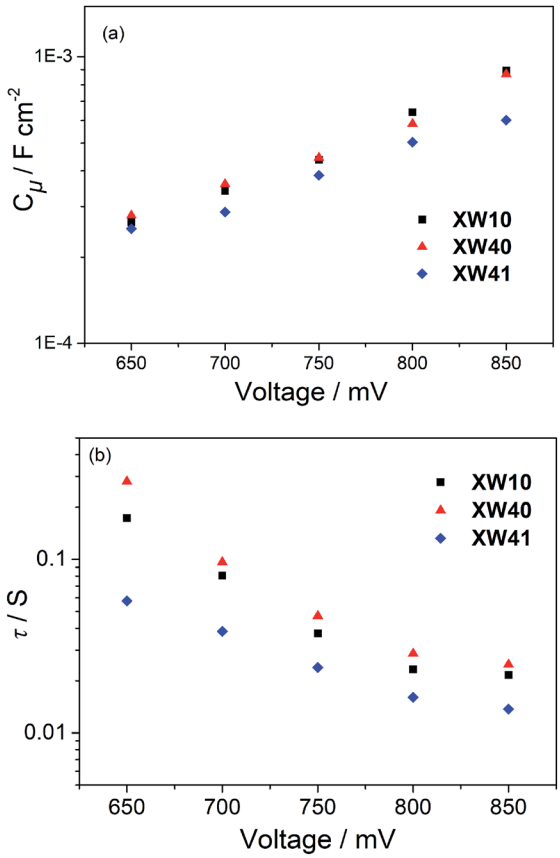

Fig. 7 Plots of (a) C_μ and (b) τ *versus* bias voltages of DSSCs based on XW10, XW40, and XW41.

porphyrin dyes. On the other hand, the C_μ values of **XW41** are lower than those of **XW40**, which is favorable for improving the V_{oc}. However, the electron lifetimes for **XW41** are much shorter than those of **XW40** which is unfavorable for the V_{oc}. As a result of the contradictory effects, **XW41** exhibits a lower V_{oc} than

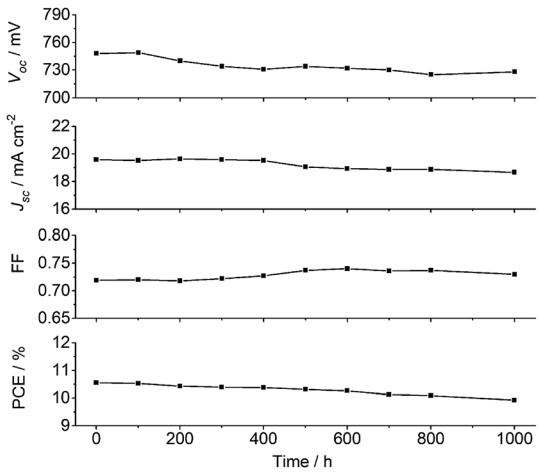

Fig. 8 Variation of the photovoltaic parameters (V_{oc}, J_{sc}, FF, and PCE) with aging time for the DSSC device based on XW40/CDCA + Z1 measured under AM 1.5 illumination (100 mW cm^{-2}) at 60 °C over 1000 h.

XW40, indicating that the V_{oc} values are predominantly governed by the electron lifetimes. These results are consistent with the more severe dye aggregation of **XW41** associated with the extended conjugation framework due to the presence of the additional BDT unit.

Photostability

In addition to high efficiency, long-term stability is a critical requirement for practical use of DSSCs. Here, the V_{oc},J_{sc}, FF and PCE values for the **XW40**/CDCA + **Z1** cells were recorded over a period of 1000 h under one sun soaking at 60 °C (Fig. 8). After 1000 h light soaking, more than 90% of the initial PCE value was retained, indicating that the DSSCs based on **XW40**/CDCA + **Z1** are photostable.

Conclusions

In summary, a new class of doubly strapped porphyrin sensitizers has been designed and successfully synthesized as DSSC sensitizers. Compared to the dyes with the porphyrin core wrapped with four long alkoxyl chains, the circle chain strapping can further suppress the dye aggregation and charge recombination. Thus, the V_{oc} was greatly improved from 711 mV (**XW10**) to 730 mV (**XW40**). Moreover, the much more compact structures of the strapped porphyrins are favorable for improving the dye loading amount, leading to the improvement of J_{sc}. With the simultaneously improved V_{oc} and J_{sc}, the efficiency of 9.3% achieved for the strapped porphyrin was found to be significantly higher than the 8.6% obtained for the wrapped dye **XW10**. The auxiliary electron-withdrawing unit BTD in **XW41** successfully extended the response spectral range with a striking onset wavelength of 830 nm in the IPCE spectra, but the extended π-conjugation framework resulted in a lowered efficiency of 8.2% because of the aggravated dye aggregation. After applying a combined approach of coadsorption with CDCA and cosensitization with **Z1**, high efficiencies of 10.6% and 10.2% were achieved for **XW40** and **XW41**, respectively. These results provide a novel strategy for developing efficient DSSCs by employing strapped porphyrin dyes.

Conflicts of interest

There are no conflicts to declare.

Acknowledgements

This work was financially supported by the Shanghai Municipal Science and Technology Major Project (Grant No. 2018SHZDZX03) and the international cooperation program of the Shanghai Science and Technology Committee (17520750100), NSFC (21472047, 21772041, 201702062, 21811530005, 21878078), Program for Professor of Special Appointment (Eastern Scholar, GZ2016006) at Shanghai Institutions of Higher Learning, Shanghai Pujiang Program (17PJ1401700), Fundamental Research Funds for the Central Universities (WK1616004, 222201717003), and Program of Introducing Talents of Discipline to Universities (B16017). The authors thank the Research Center of Analysis and Test of the East China University of Science and Technology for the help with the characterization. W. T. is grateful to the China Scholarship Council and British Council for the visiting fellowship.

Notes and references

1 C. C. Chou, F. C. Hu, H. H. Yeh, H. P. Wu, Y. Chi, J. N. Clifford, E. Palomares, S. H. Liu, P. T. Chou and G. H. Lee, *Angew. Chem., Int. Ed.*, 2014, **53**, 178–183.
2 B. O'Regan and M. Grätzel, *Nature*, 1991, **353**, 737–740.
3 C. Li, J. Zhang, J. Song, Y. Xie and J. Jiang, *Sci. China: Chem.*, 2018, **61**, 511–514.
4 A. S. Hart, B. K. Chandra, H. B. Gobeze, L. R. Sequeira and F. D'Souza, *ACS Appl. Mater. Interfaces*, 2013, **5**, 5314–5323.
5 T. Higashino, Y. Kurumisawa, N. Cai, Y. Fujimori, Y. Tsuji, S. Nimura, D. M. Packwood, J. Park and H. Imahori, *ChemSusChem*, 2017, **10**, 3347–3351.
6 T. Higashino and H. Imahori, *Dalton Trans.*, 2015, **44**, 448–463.
7 L. L. Li and E. W. Diau, *Chem. Soc. Rev.*, 2013, **42**, 291–304.
8 J. Luo, M. Xu, R. Li, K. W. Huang, C. Jiang, Q. Qi, W. Zeng, J. Zhang, C. Chi, P. Wang and J. Wu, *J. Am. Chem. Soc.*, 2014, **136**, 265–272.
9 C. L. Wang, M. Zhang, Y. H. Hsiao, C. K. Tseng, C. L. Liu, M. Xu, P. Wang and C. Y. Lin, *Energy Environ. Sci.*, 2016, **9**, 200–206.
10 J. M. Ball, N. K. S. Davis, J. D. Wilkinson, J. Kirkpatrick, J. Teuscher, R. Gunning, H. L. Anderson and H. J. Snaith, *RSC Adv.*, 2012, **2**, 6846–6853.
11 C. L. Mai, W. K. Huang, H. P. Lu, C. W. Lee, C. L. Chiu, Y. R. Liang, E. W. Diau and C. Y. Yeh, *Chem. Commun.*, 2010, **46**, 809–811.
12 J. W. Shiu, Y. C. Chang, C. Y. Chan, H. P. Wu, H. Y. Hsu, C. L. Wang, C. Y. Lin and E. W. G. Diau, *J. Mater. Chem. A*, 2015, **3**, 1417–1420.
13 F. M. Jradi, D. O'Neil, X. Kang, J. Wong, P. Szymanski, T. C. Parker, H. L. Anderson, M. A. El-Sayed and S. R. Marder, *Chem. Mater.*, 2015, **27**, 6305–6313.
14 C. Y. Lin, Y. C. Wang, S. J. Hsu, C. F. Lo and E. W. G. Diau, *J. Phys. Chem. C*, 2010, **114**, 687–693.
15 *Enzymes in Industry: Production and Applications*, ed. W. Aehle, 3rd edn, Wiley-VCH, Weinheim, 2007.
16 C. L. Wang, C. M. Lan, S. H. Hong, Y. F. Wang, T. Y. Pan, C. W. Chang, H. H. Kuo, M. Y. Kuo, E. W. G. Diau and C. Y. Lin, *Energy Environ. Sci.*, 2012, **5**, 6933–6940.
17 Q. Chai, W. Li, Y. Wu, K. Pei, J. Liu, Z. Geng, H. Tian and W. Zhu, *ACS Appl. Mater. Interfaces*, 2014, **6**, 14621–14630.
18 A. Yella, C. L. Mai, S. M. Zakeeruddin, S. N. Chang, C. H. Hsieh, C. Y. Yeh and M. Gratzel, *Angew. Chem., Int. Ed.*, 2014, **53**, 2973–2977.
19 Y. K. Eom, S. H. Kang, I. T. Choi, Y. Yoo, J. Kim and H. K. Kim, *J. Mater. Chem. A*, 2017, **5**, 2297–2308.
20 H. Song, X. Li, H. Ågren and Y. Xie, *Dyes Pigm.*, 2017, **137**, 421–429.

21 P. Brogdon, H. Cheema and J. H. Delcamp, *ChemSusChem*, 2018, **11**, 86–103.
22 H. Li, M. Fang, R. Tang, Y. Hou, Q. Liao, A. Mei, H. Han, Q. Li and Z. Li, *J. Mater. Chem. A*, 2016, **4**, 16403–16409.
23 Y. Ren, D. Sun, Y. Cao, H. N. Tsao, Y. Yuan, S. M. Zakeeruddin, P. Wang and M. Gratzel, *J. Am. Chem. Soc.*, 2018, **140**, 2405–2408.
24 Y. Liu, Y. Cao, W. Zhang, M. Stojanovic, M. I. Dar, P. Péchy, Y. Saygili, A. Hagfeldt, S. M. Zakeeruddin and M. Grätzel, *Angew. Chem., Int. Ed.*, 2018, **57**, 14125–14128.
25 J. Liu, Y. Numata, C. Qin, A. Islam, X. Yang and L. Han, *Chem. Commun.*, 2013, **49**, 7587–7589.
26 J. Liu, X. Yang, A. Islam, Y. Numata, S. Zhang, N. T. Salim, H. Chen and L. Han, *J. Mater. Chem. A*, 2013, **1**, 10889–10897.
27 M. Ikai, F. Ishikawa, N. Aratani, A. Osuka, S. Kawabata, T. Kajioka, H. Takeuchi, H. Fujikawa and Y. Taga, *Adv. Funct. Mater.*, 2006, **16**, 515–519.
28 V. Rauch, J. Conradt, M. Takahashi, M. Kanesato, J. A. Wytko, Y. Kikkawa, H. Kalt and J. Weiss, *J. Porphyrins Phthalocyanines*, 2013, **18**, 67–75.
29 C. H. Lee and E. Galoppini, *J. Org. Chem.*, 2010, **75**, 3692–3704.
30 S. Fan, K. Lv, H. Sun, G. Zhou and Z. S. Wang, *J. Power Sources*, 2015, **279**, 36–47.
31 M. W. Lee, J. Y. Kim, H. J. Son, J. Y. Kim, B. Kim, H. Kim, D. K. Lee, K. Kim, D. H. Lee and M. J. Ko, *Sci. Rep.*, 2015, **5**, 7711.
32 Y. Gao, X. Li, Y. Hu, Y. Fan, J. Yuan, N. Robertson, J. Hua and S. R. Marder, *J. Mater. Chem. A*, 2016, **4**, 12865–12877.
33 Y. Xie, Y. Tang, W. Wu, Y. Wang, J. Liu, X. Li, H. Tian and W. H. Zhu, *J. Am. Chem. Soc.*, 2015, **137**, 14055–14058.
34 Q. Xu, G. Yang, Y. Ren, F. Lu, N. Zhang, M. Qamar, M. Yang, B. Zhang and Y. Feng, *Phys. Chem. Chem. Phys.*, 2017, **19**, 28867–28875.
35 X. Li, X. Zhang, J. Hua and H. Tian, *Mol. Syst. Des. Eng.*, 2017, **2**, 98–122.
36 J. Luo, X. Wang, L. Fan, G. Li, Q. Qi, K. W. Huang, T. L. Dexter Tam, J. Zhang, Q. Wang and J. Wu, *J. Mater. Chem. C*, 2016, **4**, 3709–3714.
37 Y. Cui, Y. Wu, X. Lu, X. Zhang, G. Zhou, F. B. Miapeh, W. Zhu and Z. S. Wang, *Chem. Mater.*, 2011, **23**, 4394–4401.
38 Y. Tang, Y. Wang, X. Li, H. Ågren, W. H. Zhu and Y. Xie, *ACS Appl. Mater. Interfaces*, 2015, **7**, 27976–27985.
39 J. Liu, B. Liu, Y. Tang, W. Zhang, W. Wu, Y. Xie and W. H. Zhu, *J. Mater. Chem. C*, 2015, **3**, 11144–11150.
40 Y. Wang, B. Chen, W. Wu, X. Li, W. Zhu, H. Tian and Y. Xie, *Angew. Chem., Int. Ed.*, 2014, **53**, 10779–10783.